

Scanning Tunneling Microscopy Study of the Structure and Orbital-Mediated Tunneling Spectra of Cobalt(II) Phthalocyanine and Cobalt(II) Tetraphenylporphyrin on Au(111): Mixed Composition Films

Dan E. Barlow,[†] L. Scudiero, and K. W. Hipps*

Department of Chemistry and Materials Science Program, Washington State University, Pullman, Washington 99164-4630

Received October 8, 2003. In Final Form: January 13, 2004

Binary thin films of cobalt(II) phthalocyanine (CoPc) and cobalt(II) tetraphenylporphyrin (CoTPP) were prepared at submonolayer coverage on Au(111)/mica substrates by vapor deposition. All sample preparation and analysis were done under an ultrahigh vacuum. Scanning tunneling microscopy (STM) constant-current images of CoPc/CoTPP mixtures showed two close-packed surface structures, with different compositional percentages and some disorder. CoPc was also observed exclusively in one-dimensional chains and as single, isolated molecules below 220 K. Occupied and unoccupied orbital energy levels were identified by STM and tunnel-diode-based orbital-mediated tunneling spectroscopy. Occupied energy levels were also confirmed by ultraviolet photoelectron spectroscopy. The transient oxidation of the Co d_{z^2} orbital is identified in STM $dI/dV(V)$ curves just negative of the 0 V sample bias for both molecules. Nearly identical constant-current contours are observed over the central Co^{2+} ions of CoTPP and CoPc, indicating that the attenuation of the d_{z^2} orbital-mediated tunneling current induced by the structure of TPP relative to Pc is at most a factor of about 10. The orbital-mediated tunneling spectra of CoTPP and CoPc are distinctly different and allow these structurally similar species to be differentially identified.

Introduction

Positional assembly is the use of external manipulation to arrange atoms and molecules in a precise arrangement. In positional assembly, one requires a high degree of control over where each individual atom or molecule is placed. Photolithography and electron beam lithography are two conventional methods of two-dimensional positional assembly that do not quite reach the single-molecule scale.¹ Atomic force microscopy and scanning tunneling microscopy (STM) are also appropriate tools for positional assembly that are capable of single-molecule, even single-atom, manipulation.^{2–6} An alternative approach to the construction of materials and devices on the nanometer scale is self-assembly. Self-assembly has become an important fabrication technique in nanoscale science, and many groups are working to transform it into an effective nano-engineering tool.

In some sense, self-assembly is nothing new; biology does it all the time. Moreover, “supramolecular” chemistry has been studied for decades, showing how molecules can combine to form new noncovalent structures.^{7–9} The concept of self-assembly largely grew out of chemists’

attempts to make molecules that aggregated spontaneously into specific configurations, in the same way biological molecules form membranes and other complex structures. Of particular interest in relation to the present paper is the role of self-assembly in the formation of ordered arrays of molecules in two dimensions. A well-known example of this two-dimensional ordering is the self-assembled monolayer (SAM), an ordered molecular assembly formed by the spontaneous adsorption of a molecular species on a substrate.¹⁰ This adsorption might take place from vapor, liquid, or solution depending on the adsorbate and the surface. SAMs that order through van der Waals interactions are well-known and are represented both by vertically oriented interactions¹¹ and those that occur in the plane of the substrate.^{12–15} Recently, another type of self-assembly has been demonstrated: one similar to that used in biological systems and based on hydrogen bonding.^{16–18} For example, it has been shown that vapor codeposition of perfluorinated cobalt(II) phthalocyanine (F_{16}CoPc) and nickel(II) tetraphenylporphyrin (NiTPP) forms an ordered two-dimensional structure where each F_{16}CoPc is surrounded by four NiTPP.¹⁸

* Author to whom correspondence should be addressed. E-mail: hipps@wsu.edu.

[†] Current address: Naval Research Laboratory, Washington, DC.

(1) *Handbook of Microlithography, Micromachining, and Microfabrication*; Rai-Choudhury, P., Ed.; SPIE Optical Engineering Press: London, 1997.

(2) Binnig, G.; Quate, C.; Gerber, C. *Phys. Rev. Lett.* **1986**, *56*, 930.

(3) Kim, Y.-T.; Bard, A. J. *Langmuir* **1992**, *8*, 1096.

(4) Ross, C. B.; Sun, L.; Crooks, R. M. *Langmuir* **1993**, *9*, 632.

(5) Liu, G.-Y.; Xu, S.; Qian, Y. *Acc. Chem. Res.* **2000**, *33*, 457.

(6) Maoz, R.; Cohen, S.; Sagiv, J. *Adv. Mater.* **1999**, *11*, 55.

(7) Lehn, J. N. *Supramolecular Chemistry: Concepts and Perspectives*; VCH: Weinheim, Germany, 1995.

(8) Desiraju, G. R. *Angew. Chem., Int. Ed. Engl.* **1995**, *34*, 2311.

(9) *Comprehensive supramolecular chemistry*; Atwood, J. L., Davies, J., MacNicol, D., Votle, F., Eds.; Pergamon: New York, 1996.

(10) Ulman, A. *An Introduction to Ultrathin Organic Films: From Langmuir–Blodgett to Self-Assembly*; Academic Press: New York, 1991.

(11) Sullivan, T.; Huck, W. *Eur. J. Org. Chem.* **2003**, 17.

(12) Yablon, D.; Giancarlo, L.; Flynn, G. W. *J. Phys. Chem. B* **2000**, *104*, 7627.

(13) De Feyter, S.; Larsson, M.; Shuurmans, N.; Verkuijl, B.; Zorinians, G.; Gesquiere, A.; Abdel-Mottaleb, M.; Esch, J.; Feringa, B.; van Stam, J.; De Schryver, F. *Chem.–Eur. J.* **2003**, *9*, 1198.

(14) Yablon, D.; Guo, J.; Knapp, D.; Fang, H.; Flynn, G. W. *J. Phys. Chem. B* **2001**, *105*, 4313.

(15) Claypool, C. L.; Faglioni, F.; Goddard, W. A.; Gray, H. B.; Lewis, N. S.; Marcus, R. A. *J. Phys. Chem. B* **1997**, *101*, 5978.

(16) Hipps, K. W.; Scudiero, L.; Barlow, D. E.; Cooke, M. P. *J. Am. Chem. Soc.* **2002**, *124*, 2126.

(17) Griessl, S.; Lackinger, M.; Edelwirth, M.; Hietschold, M.; Heckl, W. *Single Mol.* **2002**, *1*, 25.

(18) Scudiero, L.; Hipps, K. W.; Barlow, D. E. *J. Phys. Chem. B* **2003**, *107*, 2903.

The growing interest in multicomponent films adds a new dimension to the self-assembly problem. If one mixes two components that independently form an ordered structure, what is the structure of the binary system? While for some applications it is desirable to have a random distribution of one in another,¹⁹ in other cases one may see internal ordering,^{20–22} phase separation,^{23–25} or even the loss of order.²⁶

van der Waals interactions in long-chain aliphatics, chemisorption in thiols and silanes, and H bonding in more compact systems can all lead to two-component self-assembly. Thus, it becomes important to ask “What role do molecule–molecule and molecule–substrate forces play in the two-dimensional structures formed from two-component thin films?” Also, given that these structures may be disordered and not amenable to conventional structure analysis, one must ask “Do methods exist to clearly identify the resulting structures and the types of molecules occupying the various sites?”

The present paper addresses both these issues for a single special case, the cobalt(II) phthalocyanine (CoPc)/cobalt(II) tetraphenylporphyrin (CoTPP) pair. This pair was chosen because they have rather similar electronic structures but significant differences in geometry. The geometry differences will produce differing substrate–molecule and molecule–molecule interactions both through van der Waals interaction and through orbital orientation relative to the gold substrate. These, in turn, will affect surface diffusion of the adsorbates and the packing and composition of the resulting self-assembled structures. The degree of adsorbate–substrate (A–S) orbital overlap should depend on both the spatial orientation and the energetics of molecular orbitals (MOs) and will certainly modify the tunneling probability. Specifically, the CoPc/CoTPP pair allows one to investigate the effect of changing the Co²⁺–Au distance on the tunneling rate through the cobalt ion. The structure of the CoTPP molecule suggests that the Co²⁺ ion should sit about 0.15 nm higher above the gold surface than Co²⁺ in CoPc. If the net tunneling rate between cobalt and gold is much greater than between tip and cobalt ion, then the constant-current contour would reflect this 0.15-nm height difference and the center of the CoTPP would appear much higher than the CoPc center. On the other hand, if the Au–CoTPP tunneling rate was greatly attenuated by the increased Co²⁺–Au distance, one would expect that the constant-current height of the Co(II) ion in CoTPP would appear much shorter than the predicted physical height, perhaps even as a depression in the center of the TPP ligand. Thus, the relative heights of the Co²⁺ ions in CoTPP and CoPc in a constant-current contour reflect the effects of distance on the cobalt–gold tunneling probability. Finally, these molecules are of interest because they have separately been studied in some detail by STM,^{27,37,45} and orbital-mediated tunneling spectroscopy (OMTS) for CoTPP has

been reported.³⁸ Also, F₁₆CoPc/NiTPP complex films are known to form.¹⁸

Experimental Section

Scanning Tunneling Methods. STM and STM-based spectroscopy analysis was done in an ultrahigh vacuum (UHV) with a commercial variable-temperature microscope (model UHV300) and control electronics (model SPM100) from RHK Technology.²⁸ The sample temperature was measured using a type K thermocouple in direct contact with the sample. Residual gas analysis of the STM chamber typically detected H₂ at $\sim 2 \times 10^{-10}$ Torr and very low levels of H₂O, CO, and CO₂ all below 2×10^{-11} Torr. These pressures were reached with a 410 L/s Starcell ion pump from Varian Vacuum Technologies.²⁹ The instrument was mounted on air legs and housed in a low-vibration laboratory at Washington State University.

STM tips were prepared from 0.25-mm W or Pt_{0.8}/Ir_{0.2} wire (purchased from Alfa Aesar³⁰ and California Fine Wire Co.,³¹ respectively). W tips were prepared by electrochemical etching, while Pt/Ir tips were prepared by mechanical cutting. At least 90% of the tips were capable of imaging Au(111) atomic steps and reconstruction corrugation, while roughly 1 in 3 were sharp enough to obtain atomic resolution on gold. Generally, several tips were made at a time and then loaded into the STM chamber, where it could be determined which tips were best by imaging Au(111). W tips always required additional cleaning by electron bombardment once in the UHV.

STM/STS Sample Preparation. A dedicated cryopumped (Cryotorr 8, 1500 L/s, CTI Cryogenics) chamber was used for the preparation of Au(111)/mica samples by vapor deposition. This chamber reached a base pressure of 8×10^{-10} Torr without baking. Mica substrates were cut from 1×4 cm sheets purchased from Ted Pella³² (Pelco #54). Freshly cleaved mica was heated at 500 °C for 24 h to remove water from the surface, and then the temperature was reduced to 380 °C for gold deposition. Gold splatters (99.999%, Cerac, Inc.)³³ were evaporated from resistively heated tungsten boats (ME5-0.005W, R. D. Mathis Co.)³⁴ that consisted of a 0.025 in. \times 0.005 in. W strip with a dimple in the center. With these boats, the pressure could be maintained in the low 10^{-9} Torr while evaporating gold at rates of ~ 0.5 Å/s over a period of ~ 1 h. The source was heated, and the deposition rate was monitored with a quartz crystal monitor until a constant value between 0.2 and 0.5 Å/s was obtained. The mica was then moved over the gold source, and the thickness of the film was calculated from the amount of time the mica was exposed to the gold vapor. About 120 nm of gold was usually deposited. The resulting Au film was allowed to cool for at least 6 h before removing and mounting on RHK sample holders. These substrates were removed from the Au deposition chamber as needed and immediately inserted into the sample preparation chamber that is attached to the RHK STM chamber. Some of the substrates used for the CoPc–CoTPP mixtures were also hydrogen flame-annealed before loading into the STM sample chamber.

Organic thin films were prepared by vapor deposition onto the Au(111)/mica substrates in the preparation chamber portion of the RHK vacuum system. These samples were then transferred to the attached STM analysis chamber. CoTPP was purchased from Frontier Scientific, Inc.,³⁵ and CoPc was purchased from Strem Chemicals, Inc.³⁶ Molecular models of CoPc and CoTPP are shown in Figure 1. CoPc was doubly sublimed under a vacuum in a quartz sublimation apparatus. Pure films of CoPc or CoTPP on Au(111) were prepared in an UHV chamber connected to the STM chamber, and the film thickness was estimated ($\pm 30\%$) with a quartz crystal thin-film monitor. CoPc and CoTPP mixed

(19) Ramachandran, G. K.; Hopson, T. J.; Rawlett, A. M.; Nagahara, L. A.; Primak, A.; Lindsay, S. M. *Science* **2003**, *300*, 1413.

(20) De Feyter, S.; Larsson, M.; Schuurmans, N.; Verkuijl, B.; Zorinians, G.; Gesquiere, A.; Abdel-Mottaleb, M.; van Esch, J.; Feringa, B.; van Stam, J.; De Schryver, F. *Chem–Eur. J.* **2003**, *9*, 1198.

(21) Yablon, G.; Giancarlo, L.; Flynn, G. W. *J. Phys. Chem. B* **2000**, *104*, 7627.

(22) Pinheiro, L. S.; Temperini, M. L. *Surf. Sci.* **1999**, *441*, 45.

(23) Stohr, M.; Wagner, T.; Gabriel, M.; Weyers, B.; Moller, R. *Adv. Funct. Mater.* **2001**, *11*, 175.

(24) Kakiuchi, T.; Iida, M.; Gon, N.; Hobara, D.; Imabayashi, S.-i.; Niki, K. *Langmuir* **2001**, *17*, 1599.

(25) Hobara, D.; Kakiuchi, T. *Electrochem. Commun.* **2001**, *3*, 154.

(26) Lei, S.; Wang, C.; Wan, L.; Bai, C. *Chi. Sci. Bull.* **2003**, *48*, 1519.

(27) Yoshimoto, S.; Tada, A.; Suto, K.; Narita, R.; Itaya, K. *Langmuir* **2003**, *19*, 672.

(28) RHK Technology, Inc., 1050 E. Maple Rd., Troy, MI 48083.

(29) Varian Vacuum Technologies, 121 Hartwell Ave., Lexington, MA 02421.

(30) Alfa Aesar, 30 Bond St., Ward Hill, MA 01835.

(31) California Fine Wire Co., P.O. Box 446, Grover Beach, CA 93483-0446.

(32) Ted Pella, Inc., P.O. Box 492477, Redding, CA 96049-2477.

(33) Cerac, Inc., P.O. Box 1178, Milwaukee, WI 53201-1178.

(34) R. D. Mathis Co., P.O. Box 92916, Long Beach, CA 90809-2916.

(35) Frontier Scientific, Inc., P.O. Box 31, Logan, UT 84323-0031.

(36) Strem Chemicals, Inc., 7 Mulliken Way, Newburyport, MA 01950-4098.

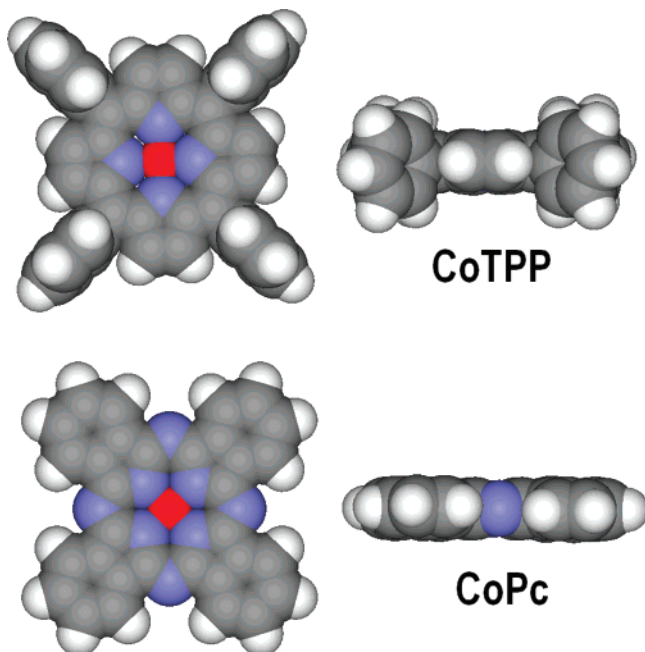


Figure 1. Top and side views of space-filled models of CoTPP and CoPc. In the color scheme, carbons are gray, nitrogens are blue, hydrogens are white, and Co(II) ions are red.

films were prepared either by first depositing 0.3 monolayer (ML) of CoPc followed by 0.5 ML CoTPP [CoPc/CoTPP] or by first depositing 0.25 MLs of CoTPP followed by 0.3 MLs of CoPc [CoTPP/CoPc]. STM-based orbital-mediated tunneling spectroscopy (STM-OMTS) was obtained from a 0.28-nm-thick CoPc (only) film on Au. dI/dV curves were numerically calculated from the average of 120 $I(V)$ data acquired at 95 K with a W tip. Similar results were also obtained using a lock-in technique and modulating the bias voltage at 5 kHz with an amplitude of +50 mV.

Ultraviolet Photoelectron Spectroscopy (UPS) Sample Preparation and Data Acquisition. UPS data were obtained with a homemade He lamp source that produces two resonance lines, He(I) (21.2 eV) and He(II) (40.8 eV), by cold cathode capillary discharge. The He lamp was set to run with a filament current of 17.0 A, voltage of +9.0 V, and He gas pressure at 250 mTorr. The discharge was adjusted to +190 V and 0.5 A. Only the 21.2 eV He(I) line was used in this study. A platinum-coated concave 600 groove/mm reflection grating with a 3.5° blaze angle coupled with a gold-coated spherical focusing mirror was used to produce monochromatic UV radiation. The base pressure in the monochromator chamber was 2×10^{-9} Torr. The UPS system is attached via a UHV valve to a Kratos Axis-165 electron spectrometer having a base pressure of 5×10^{-10} Torr.

Two different types of gold surfaces were studied. Au(111) samples (140-nm thick) made in a vacuum ($<3 \times 10^{-9}$ Torr) by vapor deposition on mica³⁷ and polycrystalline Au foil (99.985% purity). The gold foil was cleaned by heating and argon ion etching before use. The Au(111) samples were prepared exactly as just described for the STM substrates. Both types of gold were used to check the substrate work function and the calibration of the He lamp. In addition, the polycrystalline gold sample was used as the substrate for the UPS studies of the metalorganic films. CoPc and CoTPP were thermally deposited onto polycrystalline gold, in a vacuum (5×10^{-9} Torr) prep chamber attached to the UPS spectrometer. The thickness of the samples was 4 nm, as determined with a quartz crystal microbalance.

The UPS spectra were acquired using an electrostatic lens that focused the ejected electrons into the spectrometer. A bias of -20 V was applied to the sample to shift the spectra out of the nonlinear region of the analyzer (KE = 0–10 eV). The spectrometer was used in the fixed analyzer transmission mode with a pass energy of 20 eV and spatial resolution of 120 μm . The

(37) Lu, X.; Hippias, K. W.; Wang, X. D.; Mazur, U. *J. Am. Chem. Soc.* **1996**, *118*, 7197.

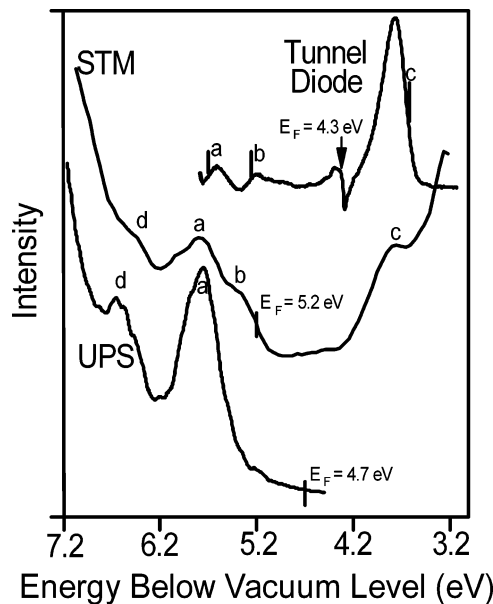


Figure 2. Combined tunneling spectroscopy and UPS results for CoPc. Energy is referenced to the vacuum level using the substrate Fermi energy. The tunnel-diode spectrum is a plot of the NTIs for an Al–Al₂O₃–CoPc–Pb tunnel diode acquired at 77 K by Mazur and Hippias.⁴² The STM-based OMT spectrum is a plot of dI/dV for CoPc on Au(111) acquired at 95 K, while the UPS is a plot of photoelectron counts for CoPc on polycrystalline Au at 298 K. The labeled peaks mark the peak DOS in the STM and UPS data, while the labeled lines mark the peak DOS for the tunnel-diode results. STM-OMTS was obtained from a 0.28-nm-thick CoPc film on Au. It is an average of 120 dI/dV curves, numerically calculated from $I(V)$ data acquired at 95 K with a W tip.

photoemitted electron energies were analyzed by a Kratos hemispherical analyzer and counted by eight-channel electron multipliers. Under these conditions, the energy resolution of the spectrometer is better than 150 meV, which was determined at the Fermi edge of an Ar-etched single crystal of Au (111).

Results

STM-OMTS, tunnel-diode-based OMTS, and UPS of CoTPP have been previously reported.³⁸ Tunnel-diode-based OMTS gives derivative-shaped peaks in $(d^2I/dV^2)/(dI/dV)$ from which the occupied and unoccupied MO energies can be extracted.³⁹ STM-based OMTS produces peaks in dI/dV (or $d \ln I/d \ln V$) that correlate with occupied (negative sample bias) and unoccupied (positive sample bias) MOs.^{37,38,40} UPS provides the energies of occupied MOs. For the excitation energy used in this UPS study, the MOs observed are primarily those derived from s- and p-type atomic orbitals. The use of these three techniques for the comparative measurement of adsorbate orbital energy levels was discussed in detail elsewhere.^{38,41} Here, we report the combined spectroscopic results for CoPc on Au(111), shown in Figure 2. The spectra are plotted relative to the vacuum level using $E_F[\text{Au}(111)/\text{mica}] = 5.2$ eV for STM-OMTS, $E_F[\text{polycrystalline Au}] = 4.7$ eV for UPS, and $E_F = 4.3$ eV for a Al–Al₂O₃–CoPc–Pb tunnel diode. The tunnel-diode OMTS⁴² was acquired at 77 K and is plotted as normalized tunneling intensity (NTI),⁴³

(38) Scudiero, L.; Barlow, D. E.; Mazur, U.; Hippias, K. W. *J. Am. Chem. Soc.* **2001**, *123*, 4073.

(39) Hippias, K. W.; Mazur, U. *J. Phys. Chem. B* **2000**, *104*, 4707.

(40) Deng, W.; Hippias, K. W. *J. Phys. Chem. B* **2003**, *107*, 10736.

(41) Scudiero, L.; Barlow, D. E.; Hippias, K. W. *J. Phys. Chem. B* **2002**, *106*, 996.

(42) Mazur, U.; Hippias, K. W. *J. Phys. Chem. B* **1999**, *103*, 9721.

(43) Hippias, K. W.; Mazur, U. *J. Phys. Chem.* **1993**, *97*, 7803.

Table 1. Comparison of Ionization Potentials and Electron Affinities by STM-OMTS, Tunnel-Diode OMTS, and UPS for CoPc and CoTPP^a

molecule	ϵ_{HOMO} (UPS)	tunnel-diode OMTS ³⁹	STM-OMTS	assignment
CoTPP occupied	6.5 ^b		6.4 ^b	$a_{1u}(\pi)$, $a_{2u}(\pi)$
		5.1	5.3 ^b	$a_{1g}(d_z)$
CoTPP unoccupied		3.4	3.5 ^b	$e_g(\pi^*)$
CoPc occupied	6.6 ^c		6.5 ^c	?
	5.8 ^c	5.7 ^d	5.8 ^c	$a_{1u}(\pi)$
		5.3 ^d	5.4 ^c	$a_{1g}(d_z)$
CoPc unoccupied		3.6 ^d	3.7 ^c	$e_g(\pi^*)$

^a Energies are in electronvolts below the vacuum level. ^b Reference 38. ^c This work. STM-OMTS = $dI/dV(V)_z$, submonolayer film on Au(111)/mica. ^d Reference 42.

or $(d^2I/dV^2)/(dI/dV)$. A correction was used to determine the peak density of states (DOS) in the tunnel-diode spectrum, as described in ref 39. The STM-OMTS was acquired from a submonolayer of CoPc on Au(111)/mica, with the tip positioned over the CoPc molecules on the sample. The STM data is an average of 120 $dI/dV(V)_z$ curves, numerically calculated from $I(V)$ data acquired at 95 K with a W tip. The He(I) UPS displayed is from a multilayer film (about 10 ML) on polycrystalline gold foil acquired at room temperature. STM-OMTS and tunnel-diode OMTS probe both occupied and unoccupied orbitals, but conventional single-photon UPS probes occupied orbitals only. STM and tunnel-diode spectra show peaks in the DOS at about 5.8 (a), 5.4 (b), and 3.7 (c) eV. UPS also reveals a peak at about 5.8 eV (a) and a peak at 6.6 eV (d), in agreement with an additional peak in the STM-OMTS at 6.5 eV (d). This last peak was outside the range of the tunnel-diode OMTS. These results are summarized in Table 1.

With a coverage of only 0.4 ML of CoPc on Au(111), no molecules could be observed at room temperature by STM as a result of surface diffusion of the molecules. CoPc was only observed at room temperature at coverage values greater than or equal to 0.6 ML. A similar observation was reported for CuPc on single-crystal Au(111).⁴⁴ However, CoTPP at ~ 0.4 ML coverage on Au(111) can be imaged by STM at 295 K.^{38,45} At 0.4 ML coverage, pure CoTPP is observed in close-packed islands with an approximately square unit cell.

Figures 3 and 4 show low-resolution constant-current STM images of CoPc/CoTPP and CoTPP/CoPc mixed films. The images were acquired at 295 K. Two types of compositionally disordered, close-packed structures are observed at 295 K (Figures 3 and 4). The surface structure of regions A and B in Figure 3 appears hexagonal (actually rectangular) and contains a nearly 50/50 mix of CoPc and CoTPP, as determined by high-resolution imaging of these structures. This same structure can be seen in the lower right of the CoTPP/CoPc STM image (Figure 4). Region C in Figure 3 and the lower left region in Figure 4, has fourfold symmetry. These fourfold structures are typically at least 80% CoTPP. At the sample bias (-0.8 V) used in Figure 3, the CoPc molecules can be identified as the slightly "brighter" dots. This apparent height is due to enhanced orbital-mediated tunneling (OMT) via the highest occupied π orbital of the Pc ligand relative to that of the TPP. OMTS results for CoTPP place the highest occupied π orbital at about -1.25 V,³⁸ while the current study places the highest occupied π of CoPc near -0.7 eV (relative to the Fermi energy). Thus, at -0.8 -V bias the

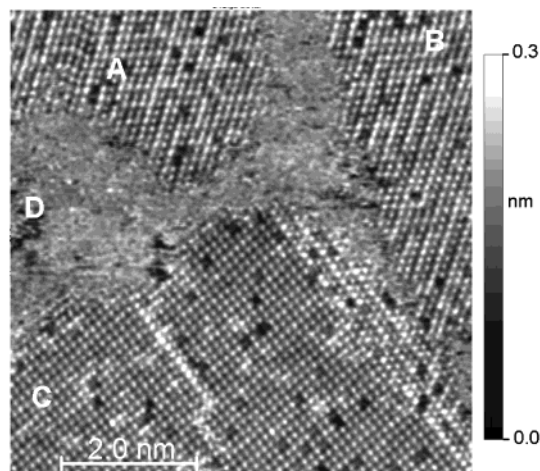


Figure 3. STM constant-current image of a CoPc/CoTPP mixture, $T = 295$ K. A total of 0.3 ML of CoPc was first deposited on Au(111) followed by 0.5 ML of CoTPP. Acquired with a Pt/Ir tip at a setpoint with a -0.8 -V sample bias and 0.05 nA. The image was flattened.

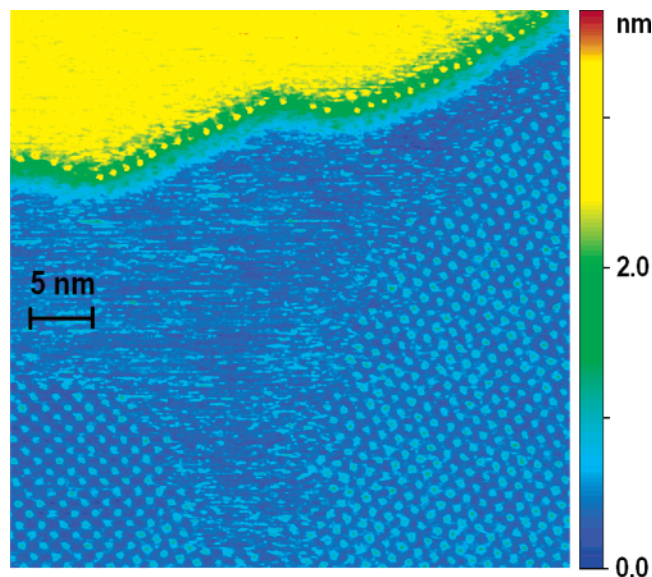


Figure 4. STM constant-current image of a CoTPP/CoPc mixture, $T = 295$ K. A total of 0.25 ML of CoTPP was first deposited on Au(111) followed by 0.3 ML of CoPc. Acquired with a W tip at a setpoint with a -0.4 -V sample bias and 0.10 nA.

highest occupied π of CoPc is closer to resonance than the corresponding CoTPP orbital. Figure 4 was acquired at -0.4 V bias, near resonance with the half-filled d_z orbital in both complexes (vide infra). Thus, it is difficult to distinguish the two molecules at this bias.

Two additional features deserve mention. Region D in Figure 3 and the upper and mid-regions of Figure 4 appear to be molecule-free. In fact, as we will show, these are regions of low molecular density where the molecular diffusion rate is faster than the STM imaging time. It is also interesting that the step edge in Figure 4 is occupied by molecules. Pure CoTPP on Au(111) shows a strong preference for step-edge adsorption at ~ 0.4 ML coverage at room temperature, while pure CoPc forms no ordered regions until about 0.6 ML. Thus, it seems likely that the molecules on the step edges are CoTPP and that CoPc can only be imaged at 295 K and ≤ 0.4 ML when imbedded in a CoTPP matrix.

Figure 5 shows that when the sample is cooled from 295 to 176 K, molecules occupying the "noisy" regions are

(44) Chizhov, I.; Scoles, G.; Kahn, A. *Langmuir* **2000**, *16*, 4358.

(45) Scudiero, L.; Barlow, D. E.; Hipps, K. W. *J. Phys. Chem. B* **2000**, *104*, 11899.

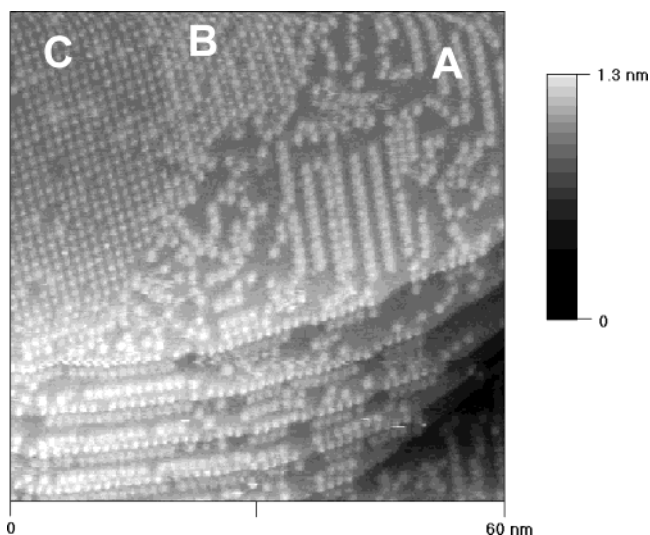


Figure 5. STM constant-current image of a CoPc/CoTPP mixture at $T = 176$ K. A total of 0.3 ML of CoPc was first deposited on Au(111) followed by 0.5 ML of CoTPP. The image was acquired using a W tip at setpoint with a -0.8 -V sample bias and 0.1 nA and was flattened. The top portion of the image shows distortion due to piezo creep.

frozen on the surface. The regions between the close-packed structures that appeared noisy at 295 K in Figures 3 and 4 clearly contain a lower density of molecules that can be “frozen” on the Au surface at 176 K (region A of Figure 5). On the flat terraces in region 5A, linear chains, clusters, and single molecules are observed. By using OMTS, the molecules in region 5A are identified as CoPc, exclusively. We also observe linear chains at a low temperature on pure CoPc–Au(111) samples. On pure CoTPP–Au(111), either islands or single scattered molecules were observed, but linear chains were not seen. Figure 5 also shows that adsorbates on this surface have an affinity for step edges. Bias-dependent imaging indicates that a row of CoTPP aggregates right on the step edge, followed by a second (inner) row of CoPc molecules. This result is especially interesting because CoPc was deposited first in this sample. Moreover, it is consistent with our interpretation of the 295 K image: CoTPP forms on the step edges at room temperature and CoPc cannot displace it as the sample cools.

The CoPc linear chains that appear on the terraces at 176 K are stabilized at higher temperatures by higher surface coverage. As shown in Figure 6, at 295 K stable CoPc one-dimensional chains can be seen on pure CoPc films having a coverage of about 0.7 ML on Au(111)/mica. Here, one-dimensional chains extending over 30 molecules as well as shorter chains separated by kinks are observed. The image shows two preferential orientations of the rows with an angle of $135 \pm 5^\circ$ between them. Further analysis of the data files shows that the CoPc one-dimensional rows exist at relative orientations of 15° multiples. Other observations of chainlike phthalocyanine aggregates have been reported for submonolayer coverage of SnPc on HOPG,⁴⁶ CuPc on HOPG,⁴⁶ and SnPc on Ag(111).⁴⁷ The CoPc–Au(111) chainlike structures reported here show longer-range order.

It is also interesting to note that CuPc is known to preferentially orient along step edges at ML coverage.⁴⁴ However, Chizhov et al. did not see single rows of molecules isolated at step edges. Further, their explanation for the

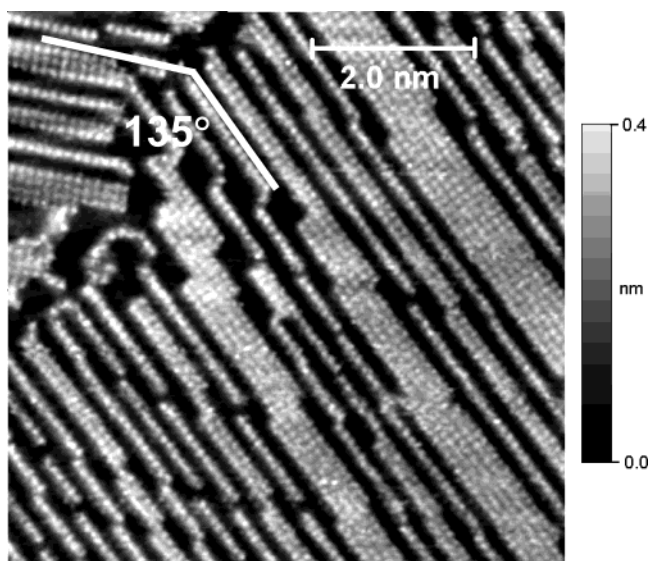


Figure 6. Approximately 0.7 ML of the pure CoPc/Au(111) sample in a region with the one-dimensional rows. Acquired at 295 K with a W tip, $+0.8$ -V sample bias, and 0.1 nA setpoint. The image was flattened.

preferred step-edge orientation, which involved maximizing the area covered on short terraces, does not apply to the single line adsorption seen here. Chizhov et al. also reported that CuPc did not form ordered films at submonolayer coverage.

Figure 7 presents the high-resolution STM image of a phase-segregated CoTPP/CoPc mixed region and an ordered region containing only CoTPP. The molecules can be identified by shape. The CoTPP molecules look rounded, and CoPc has a four-leaf-clover shape. The apparent high spots in the centers of the molecules are due to enhanced tunneling via the half-filled d_{z^2} orbitals present in both CoPc and CoTPP.^{37,38,48,49} The symmetry and lattice spacing of the two regions in Figure 7 are the same as the ones in Figures 3 and 4. The mixed region (lower part of the figure) shows a preference for alternating CoPc/CoTPP molecules, but some disorder is present.

The CoTPP-only regions have a unit cell angle of $90 \pm 5^\circ$ and lattice spacing of 1.35 ± 0.15 nm. In the mixed region in Figure 7, a row of mostly CoPc is at the interface with the CoTPP-only region. The next row of molecules in the mixed region, below the first CoPc row, is mostly CoTPP. The rows continue to alternate between mostly CoPc and mostly CoTPP. A model of this surface structure is shown in Figure 8. The lattice spacing for rows with nonalternating molecules is 1.35 ± 0.15 nm: the same as the spacing in the CoTPP-only region. The lattice spacing for rows with alternating molecules is 1.50 ± 0.15 nm. The angle between an alternating and nonalternating row, α , is $63 \pm 5^\circ$, and the angle between two nonalternating rows, β , is $54 \pm 5^\circ$. Thus, the surface has a rectangular unit cell with two molecules per cell and a unit cell angle of $\alpha + (1/2)\beta = 90^\circ$.

The significance of the applied bias in Figure 7 ($+0.4$ V) can be understood by considering Figure 9. Figure 9 presents the STM-OMTS obtained from pure samples of CoPc and of CoTPP on Au(111) at 298 K. The energies relative to the vacuum level were determined by taking

(46) Walzer, K.; Hietschold, M. *Surf. Sci.* **2001**, *471*, 1.

(47) Lackinger, M.; Hietschold, M. *Surf. Sci.* **2002**, *520*, L619.

(48) Hipps, K. W.; Lu, X.; Wang, X. D.; Mazur, U. *J. Phys. Chem.* **1996**, *100*, 11207

(49) Lu, X.; Hipps, K. W. *J. Phys. Chem. B* **1997**, *101*, 5391.

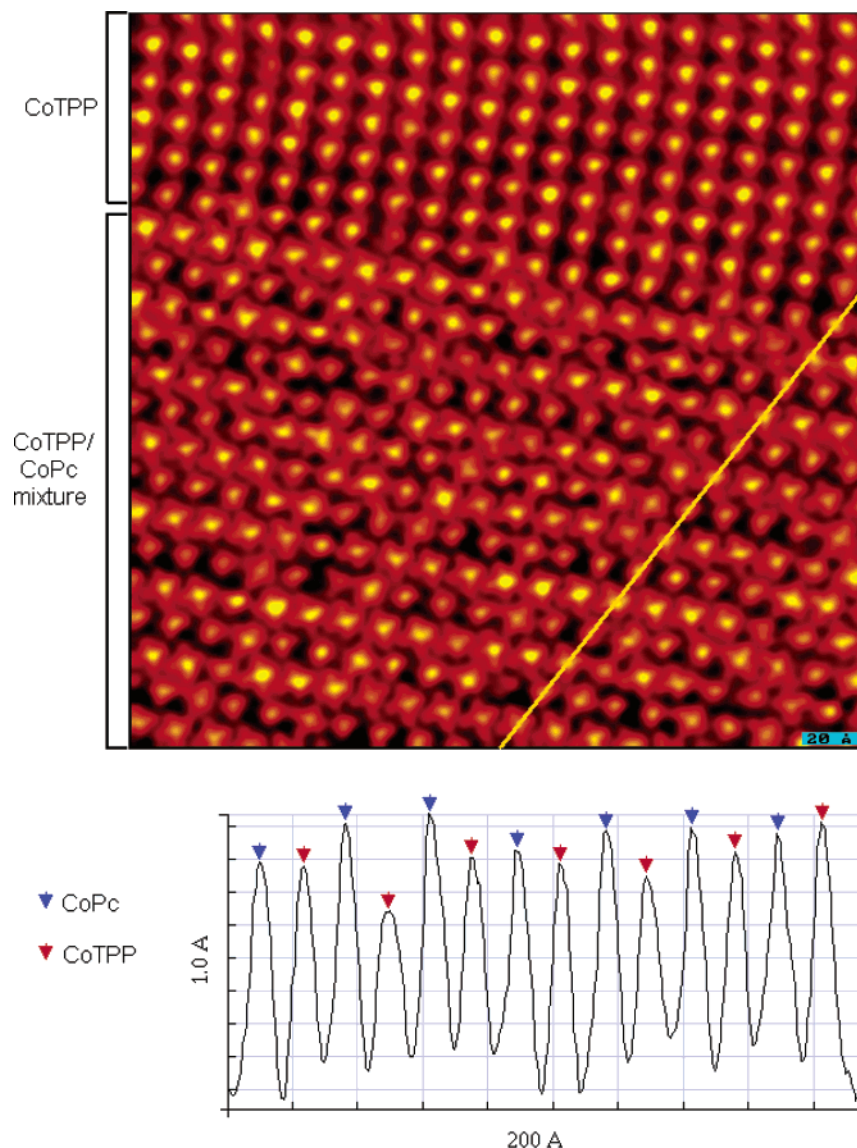


Figure 7. High-resolution constant-current STM image of CoTPP and CoPc on Au(111)/mica. The CoTPP/CoPc film was made by first depositing 0.25 ML of CoTPP on Au(111) followed by 0.3 ML of CoPc. Acquired with a W tip, +0.4 V sample bias, 0.1 nA, and 295 K. The molecules can be identified by their appearance, where CoTPP appears rounded and CoPc has a four-leaf-clover shape. A line profile that goes through an alternating series of CoPc and CoTPP molecules is also shown. The image was plane-fit, low-pass-filtered, and median-filtered.

the Fermi energy to lie at 5.2 eV. A sample bias of +0.4 V places the Fermi energy of the tunneling electron near 4.8 eV, as shown in the figure. At this bias, the majority of the tunneling current is energetically out of resonance with all the orbitals of both molecules. Moreover, the $\text{Co}^{2+} \Rightarrow \text{Co}^{3+}$ transient oxidation in both complexes lies about +0.5 V away. Thus, one expects that relative resonance energy factors will not play a role in the imaging. However, the relative coupling of the d_z orbital of the complexes to the tip or substrate still will be significant. Thus, the centers of the CoTPP molecules should look dimmer (in a constant-current image) than the centers of CoPc if the CoTPP d_z orbital lies physically farther from the Au surface than that of the CoPc.

A sectional profile that goes through an alternating row of CoTPP/CoPc molecules, indicated as a yellow line in the image, is plotted below the image in Figure 7. In the section shown, the heights of both CoPc and CoTPP reflect the apparent height of the central Co(II) ion. These heights vary across the image but suggest that the CoPc is "higher" than CoTPP. This variation in apparent height is due in part to the underlying gold reconstruction and also to small

fluctuations in molecular positions. To obtain a significant measure of the relative heights, a large number of individual molecules in Figure 7 were measured. On the basis of this averaging, a height difference of 0.03 ± 0.04 nm was obtained with Co^{2+} in CoPc being marginally taller than in CoTPP. Another method was to use the RHK correlation software to extract an average sectional contour for individual CoPc and CoTPP molecules. This method also led to very similar heights for the two compounds (within ± 0.02 nm).

Discussion

The STM and UPS results and assignments for CoPc and CoTPP are summarized in Table 1. The peak near 5.3 eV observed in the tunnel-diode and STM-OMTS but not in the UPS is assigned to the transient oxidation of the half-filled d_z orbital on the Co(II) ion. This peak was not observed in UPS because He(I) UPS is much more sensitive to s and p orbitals than to d orbitals. The peak near 5.8 eV is observed with all three techniques and is assigned to the oxidation of the π highest occupied molecular orbital, while the peak at 3.7 eV is assigned to the reduction of

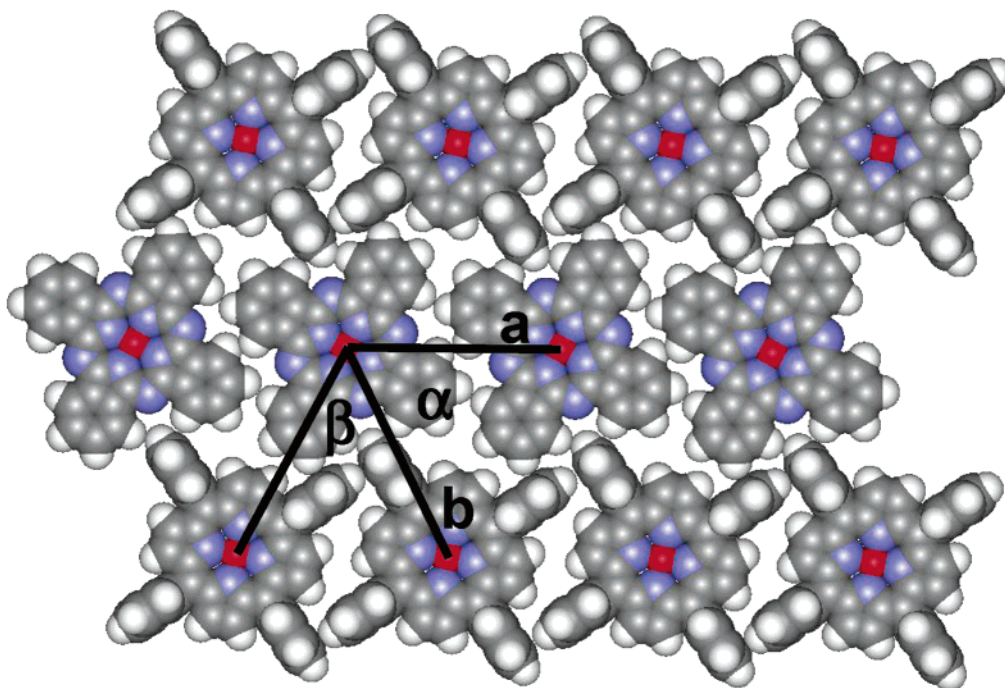


Figure 8. Model of the preferred surface structure of the mixed regions. Lattice spacings are $a = 1.35 \pm 0.15$ nm along rows with nonalternating molecules and $b = 1.50 \pm 0.15$ nm along rows with alternating molecules. Two different angles are possible between adjacent rows. The angle α , between rows with alternating and nonalternating molecules, is $63 \pm 5^\circ$. The angle β , between two rows with molecules that alternate, is $54 \pm 5^\circ$.

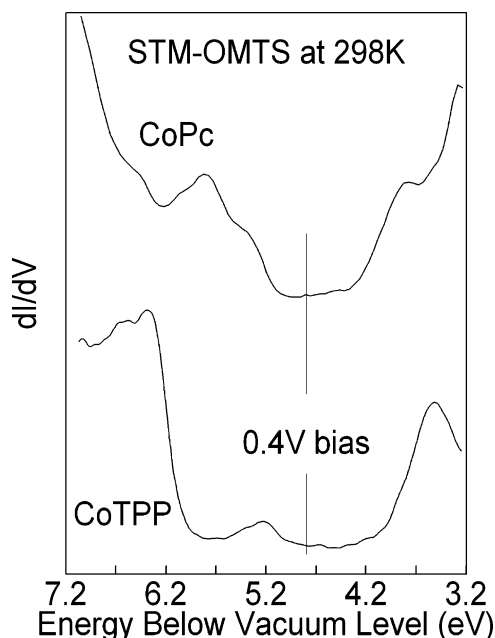


Figure 9. STM-OMTS of CoPc and CoTPP at 298 K. Zero bias is taken as 5.2 eV relative to the vacuum level. The bias at which Figure 6 was acquired (+0.4 V) is indicated on the graph.

the π^* LUMO. These assignments are consistent with electrochemical redox potentials.⁴² The MO designations are based on the calculations by Rosa and Baerends.⁵⁰ The UPS and STM-OMTS peak near 6.5 eV (peak d in Figure 2) is not assigned here.

The CoPc/CoTPP mixture on Au(111) provides an interesting binary system for studying the surface structures that result from two “miscible” adsorbates with different A–S and adsorbate–adsorbate (A–A) interaction strengths. STM imaging of the pure components showed

that CoTPP–CoTPP interaction energies exceed those for CoPc–CoPc. CoPc remains in motion on Au(111) at 295 K when the coverage is ~ 0.5 ML, while CoTPP molecules form ML islands.^{38,45} Thus, that A–A interactions are stronger for CoTPP.

While there might also be a small enhancement of the CoTPP island formation from preferential Au–CoTPP interactions, these are at best weak on terraces because no where are single molecules or small clusters observed on the Au terraces. One expects the Au–CoTPP interaction to be weak on terraces because the CoTPP–Au contact is only through the perpendicular phenyl rings, as shown in Figure 1. Thus, it is surprising that the CoTPP–Au interaction is stronger than the CoPc–Au interaction at the step edges. Even on the terraces, the CoPc–Au interaction, which should be stronger than the CoTPP–Au interaction, is weak because single molecules are never localized on Au at room temperature and ordered chains and islands only appear at higher coverage, as shown in Figure 6. STM imaging of pure CoPc and CoTPP on Au(111) demonstrate that the CoTPP–Au and CoPc–Au interaction energies are weak enough for surface diffusion of single adsorbed molecules at 295 K.⁴⁵

It is concluded that, during the preparation of the mixed sample, the first species deposited (either CoPc or CoTPP) diffuses across the surface, with a fraction of the molecules forming islands in the case of CoTPP. Even for CoTPP, there is a “solid–fluid” equilibrium process that is constantly changing the size of the islands. When the second compound is added, three regions are observed. A nearly square array of molecules composed mostly of CoTPP and matching the lattice spacing of pure CoTPP on Au forms because of the strong CoTPP–CoTPP interactions. A mixed composition region of rectangular symmetry and consisting of about a 1:1 ratio of CoPc and CoTPP forms driven by entropy and the fact that CoTPP–CoPc interactions exceed the CoPc–CoPc interactions. Finally, the “two-dimensional–fluid” phase is primarily composed of the excess CoPc molecules with

(50) Rosa, A.; Baerends, E. J. *Inorg. Chem.* **1994**, *33*, 584.

a small contribution from CoTPP. It is possible that the surface structures and composition ratios will change if different sample preparation conditions are used. Preparation factors include the total and relative amounts of CoPc and CoTPP deposited, the order of deposition, substrate temperature during deposition, and postdeposition annealing.

As shown by Figure 1, CoPc should be in close contact with the Au(111) surface while the porphyrin ring and central Co(II) ion of CoTPP should be roughly 0.15 nm further from the surface because of the perpendicular orientation of the phenyl groups. While the perpendicular orientation of the phenyl rings should result from strong steric hindrance and has been verified for single-crystal CoTPP⁵¹ and for metal–TPP (MTPP) complexes on Au,^{16,18,27} this is not apparent in the STM image in Figure 7. Nevertheless, we believe that the phenyl rings are more nearly perpendicular than flat for the pure CoTPP-on-Au case. Rotation of the phenyl ring to a parallel orientation should be accompanied by a geometrical distortion of the porphyrin ring. This would also cause a change in the electronic energy levels. If the phenyl group configuration relative to the porphyrin ring changed significantly on the gold surface, multilayer CoTPP films, where the phenyl groups are known to be perpendicular to the porphyrin ring, would have different electronic energies than ML films. The good agreement between the STM-OMTS, tunnel-diode OMTS, and UPS results for CoTPP shown in ref 38 supports the assumption that the CoTPP phenyl rings are perpendicular in ML films on Au(111). This is because the UPS and tunnel-diode OMTS were done on multilayer films while the STM-OMTS was taken from submonolayer coverage samples. This argument cannot be made for the CoTPP configuration in the mixed composition region. In fact, it is quite possible that the phenyl group configuration changes to optimize packing with the CoPc.

It should also be noted that in the ordered 1:1 structure formed by NiTPP and F₁₆CoPc one clearly sees that the phenyl rings are nearly perpendicular to the Au surface.¹⁸ On a cursory examination, this well-ordered structure is very different from that of the CoTPP/CoPc mixed structure reported here. In the NiTPP/F₁₆CoPc case, four F₁₆CoPc nearest neighbors surround each NiTPP, and the unit cell is rectangular. In the CoTPP/CoPc regions of near a 1:1 composition, long rows of identical molecules predominate with rectangular unit cells. On closer examination, however, there are similarities between the CoTPP/CoPc system and the NiTPP/F₁₆CoPc system. The fluorinated system is also composed of alternating rows of molecules, but the packing is much tighter. Thus, the rectangular structure seen in the case of NiTPP/F₁₆CoPc may be thought of as a tightening of the structure in CoTPP/CoPc that is driven by H bonding.

In the case of NiTPP/CoPc films formed by codeposition, a solid solution is observed. This is very different from either of the ordered MTPP/CoPc structures discussed previously. These differences in structure may be due to the deposition methods used. In the present study, the deposition was sequential, while the NiTPP/CoPc films were made by simultaneous deposition. In the case of simultaneous deposition, differing molecules may be easily trapped in growing islands. Very recently, Itaya and co-workers⁵² have reported a mixed CoPc/CuTPP film on gold deposited from benzene solution. In this case of simul-

taneous deposition, a rectangular unit cell with alternating rows of CoPc and CuTPP also is observed.

The structure differences seen in the mixed MTPP/MPc films may be due partially to differences in the central metal ion. STM images of NiTPP/CoTPP and CuPc/CoPc mixtures on the Au(111) surface show that these molecules have similar interaction strengths.^{37,45,48} VOPc on Au(111) showed a much higher affinity for island growth on Au than that observed for CoPc.^{53,54} High-resolution images of stable VOPc islands at ~0.5 ML coverage could be routinely imaged at 295 K. Also, the film formed from the sequential deposition of 0.5 ML CoPc followed by 0.5 ML VOPc is a bilayer (VOPc on top) with disordered regions consisting of a mixture of VOPc and CoPc.⁵⁴

Another motivation for comparing CoPc and CoTPP is to determine if the increased Co–Au distance inhibits the d_z OMT. As shown by Figure 7, the d_z OMT is contributing strongly in both CoTPP and CoPc, as shown by the apparent height of the molecular centers. The line profile indicates that, within the height variability of the image, the Co(II) ion has roughly the same apparent height in both the phthalocyanine and porphyrin complexes. When tunneling through the metal d_z orbital is quenched, an apparent hole is observed over the central metal ion, as for CuPc,³⁷ NiPc,⁴⁹ and NiTPP.⁴⁵ If the structure models in Figure 1 are correct, and if tunneling through the metal d_z orbital is not affected by the additional Co–Au separation in CoTPP, then one would expect the CoTPP to appear about 0.15-nm taller than CoPc at +0.4 V bias.

The true situation is clearly intermediate between these extremes. Extracting quantitative values for the reduction in Co–Au coupling in CoTPP relative to CoPc is complicated by the uncertainty in the true conformation of CoTPP on the Au surface. One can, however, estimate the attenuation in tunneling probability based on models for the transfer process. If a two-step model is chosen, the analysis proceeds as follows. At +0.4 V bias, the tunneling process is far from resonance. At steady state, therefore, one may assume that there is no net charge buildup (or loss) on the molecule. Thus, the *net* rate of electron transfer from tip to the Co²⁺ center on the molecule, $k(t-M)$, must equal the *net* rate of transfer from the Co²⁺ center of the molecule to the Au substrate $k(M-Au)$ at fixed tunneling current. The observed tip-to-molecule current–distance dependence over either adsorbate is roughly given by $I \propto e^{-1.5z}$, where z is the distance from the gold surface to the tip measured in angstroms, when z is greater than the molecule–Au separation. The constant-current contour indicates that the apparent height of the Co²⁺ in CoTPP is about the same as, and perhaps as much as 0.03 nm less than, the Co²⁺ in CoPc. On the basis of the model in Figure 1, the true height could be as much as 0.15-nm greater. That is, $k(t-CoTPP) = k(CoTPP-Au) = k(CoPc-Au)$ when the tip is about 0.18-nm closer to the Co²⁺ ion of CoTPP than to the Co²⁺ ion of CoPc. Taking the observed tunneling current to be proportional to the steady-state value of $k(t-M)$, $k(CoTPP-Au)/k(CoPc-Au) = k(t-CoTPP)/k(t-CoPc) \approx \exp(-1.5 \times 1.8) \sim 0.1$. Thus, the d_z OMT through CoTPP is attenuated by no more than a factor of about 10 relative to CoPc. If, instead, one assumes a single tunneling event with an overall exponential distance dependence in tunneling probability, one comes to a similar conclusion. The important point here is not the exact value (which is only an estimate) but the fact that the net electron-transfer rate from the molecule to the gold substrate is still very large. To see a significant

(51) Stevens, E. D. *J. Am. Chem. Soc.* **1981**, *103*, 5087.

(52) Suto, K.; Yoshimoto, S.; Itaya, K. *J. Am. Chem. Soc.* **2003**, *125*, 14976.

(53) Barlow, D. E.; Hipps, K. W. *J. Phys. Chem. B* **2000**, *104*, 5993.

(54) Barlow, D. E.; Hipps, K. W. *Ultramicroscopy* **2003**, *97*, 47.

decrease in this rate, a much larger gap between the cobalt ion and the surface must be established.

Conclusions

Coadsorption of CoPc and CoTPP onto Au(111) provides an example of how incorporation of different molecule–molecule and molecule–substrate interaction energies can lead to new supramolecular structures. Differences in the electronic structure of the two adsorbates were identified by OMTS, and these differences, in addition to differences in internal structure, can be used to distinguish the components of CoPc/CoTPP mixtures at the single-molecule level. An approximately 1:1 CoTPP/CoPc structure is seen to form spontaneously on Au(111) at low coverage irrespective of which species is deposited first. It involves the (approximate) formation of alternating rows of each complex. This structure is highly defective, and the rows are much less dense than in the stable alternating-row structure that can be generated through the use

of H–F bonding as seen in the case of NiTPP/F₁₆CoPc films.¹⁶ It is also noted that changes in the central metal ion may affect the ordering in self-assembly.

Another important issue addressed in this study was the effect of decreasing orbital overlap of an “atomic wire”: the central Co(II) ion with a Au electrode. The results show, qualitatively, that increasing the substrate–redox center distance by an estimated 0.15 nm still leaves the Co(II) ion strongly coupled with the Au substrate but that the net Co–Au electron-transfer rate is attenuated by about 1 order of magnitude.

Acknowledgment. We thank the National Science foundation for support in the form of Grants CHE 0138409 and CHE 0234726. Acknowledgment also is made to the donors of the Petroleum Research Fund, administered by the American Chemical Society.

LA035879L